Mesenchymal stem cells combined with biphasic calcium phosphate ceramics promote bone regeneration

T. L. LIVINGSTON, S. GORDON, M. ARCHAMBAULT*, S. KADIYALA, K. MCINTOSH, A. SMITH, S. J. PETER
Osiris Therapeutics, Inc., 2001 Aliceanna Street, Baltimore, MD 21231, USA
E-mail: marchambault@osiristx.com

The reconstruction and repair of large bone defects, resulting from trauma, cancer or metabolic disorders, is a major clinical challenge in orthopaedics. Clinically available biological and synthetic grafts have clear limitations that necessitate the development of new graft materials and/or strategies. Human mesenchymal stem cells (MSCs), obtained from the adult bone marrow, are multipotent cells capable of differentiating into various mesenchymal tissues. Of particular interest is the ability of these cells to differentiate into osteoblasts, or bone-forming cells. At Osiris, we have extensively characterized MSCs and have demonstrated MSCs can induce bone repair when implanted *in vivo* in combination with a biphasic calcium phosphate, specifically hydroxyapatite/tricalcium phosphate. This article reviews previous and current studies utilizing mesenchymal stem cells and biphasic calcium phosphates in bone repair.

Introduction

Mesenchymal stem cells (MSCs) are multipotent cells that are capable of differentiating along several lineage pathways [1–3]. From a small bone marrow aspirate, MSCs can be isolated and expanded into billions of cells [4–6]. Additional characterization has also identified a panel of cell surface markers and extracellular matrix molecules characteristic of the MSC [1, 7]. *In vitro* and *in vivo* analyzes have demonstrated culture expanded MSCs can differentiate into osteoblasts, chondrocytes, adipocytes, tenocytes, and myoblasts.

MSCs have been studied extensively to characterize their differentiation along the osteoblastic lineage [3, 8]. *In vitro* culture conditions containing dexamethasone, L-ascorbic acid-2-phosphate, and β-glycerophosphate demonstrated consistent MSC differentation marked by morphology, alkaline phosphatase and osteocalcin expression, and mineralization of the extracellular matrix. These characteristics were also displayed by MSC populations that had been taken out to 15 passages [1] as well as MSCs that had been cryopreserved and thawed for analysis. Maintenance of the capacity to differentiate and proliferate following cryopreservation suggests that MSCs may be valuable as a readily available and abundant source of cells in the tissue engineering field.

Large bone defects often occur as a result of trauma, cancer, or metabolic diseases. These defects are addressed in over one million reconstructive surgery cases per year [9]. Surgeons typically reconstruct these sites with biological or synthetic grafts. Autologous bone grafts, wherein bone is transferred from another site in the patient's body, are highly regarded for their osteoinductivity, established vasculature and no potential for disease transmission, but are limited due to the availability of a sufficient amount of tissue to harvest, morbidity at the harvest site, and difficulty in shaping the harvested autograft bone to fit the defect [10, 11]. Allograft bone, or tissue harvested from a cadaver, while more readily available, may carry with it the risk of disease transmission and is also difficult to shape [12–15]. A significant additional limitation of allograft bone is the delayed remodeling by the host. In the case of very large defects, the allograft may remain in the implant site throughout the patient's life, creating an area more prone to fracture or infection.

Bioactive ceramics, namely hydroxyapatites (HA), hydroxyapatite/tricalcium phosphates (HA/TCP) and bioactive glasses, have been used as scaffolds for bone reconstruction for many years [16–18]. They are termed ''bioactive'' because they form an interfacial bond with tissues upon implantation and enhance bone tissue formation as result of surface modification when exposed to interstitial fluids. They also demonstrate superior osteoconductive properties and proven biocompatibility. While these ceramics have been employed in long bone reconstruction preclinically [19–22], most preclinical and clinical applications are in the area of craniofacial,

*Author to whom all correspondence should be addressed.

dental, and other non to low weight bearing skeletal site reconstructions [23–26]. Due to their brittle mechanical properties, they lack the structural integrity necessary for stability while bone ingrowth occurs for long bone repair [27, 28]. Enhancing the rate of bone formation within the ceramic implant may provide added stability to the implant and allow for rapid restoration of the mechanical integrity at the defect site. Thus, we propose long bone reconstruction can be achieved by increasing the rate of bone formation by the implantation of mesenchymal stem cells in combination with bioactive ceramics, specifically biphasic calcium phosphates.

We performed analysis *in vivo* to demonstrate this phenomenon. A standard *in vivo* osteogenesis assay was developed in which MSCs were seeded onto HA/TCP and implanted subcutaneously on the back of immunocompromised mice [5]. Histological evaluation exhibited consistent bone formation in implants seeded with MSCs, whereas the cell-free implant rarely displayed significant bone formation. The potential feasibility of MSC-based bone regeneration was then established, and extensive experimentation has subsequently confirmed MSC-directed bone formation utilizing bioactive ceramics in many *in vitro* and *in vivo* models and applications at Osiris as well as other institutions [29–31]. This paper reviews data generated and previously published at Osiris on MSC-based bone regeneration *in vivo* as well as describes additional unpublished data investigating new approaches in bone tissue engineering utilizing MSC technology.

MSC isolation and expansion

Mesenchymal stem cells are found at a frequency of approximately 1/100,000 nucleated cells in bone marrow. Osiris Therapeutics has developed methods whereby this small, distinct population can be isolated and expanded, creating multiple therapeutic doses from one small aliquot of bone marrow [32]. This isolation and expansion procedure has been validated with over 600 human donors, as well as animal species including baboon, goat, canine, rabbit, and rat. The experiments described in this manuscript utilize rat, canine, or human MSCs as specified. In brief, for human MSC production bone marrow aspirates of 30–50 mL were obtained from healthy adult donors. Marrow samples were washed with saline, followed by centrifugation over a density cushion. The interface layer was removed, washed, and cell counts were performed. Nucleated cells recovered from the density separation were washed and plated in tissue culture flasks in Dulbecco's Modified Eagle's Medium (DMEM) containing 10% fetal bovine serum (FBS). The FBS was obtained from HyClone Laboratories, Inc., which performs extensive virus testing and obtains their fetal bovine blood from USDA inspected abattoirs located in the United States. Non-adherent cells were washed from the culture during biweekly feedings. Colony formation was monitored for a 14–17 day period. When the tissue culture flasks were near confluent, the MSCs were passaged. At the end of the first passage, MSCs were enzymatically removed from the culture flask using trypsin-EDTA and replated at a lower density for further expansion. At the end of the second passage, MSCs were either seeded onto scaffolds or cryopreserved until future use. Similar methods were used to prepare rat and canine MSCs for scafffold seeding and evaluation of their osteogenic potential in the orthotopic models described. Similar methods were employed for the growth of MSCs from other species.

Critically-sized femoral defects in the rat: rat and human MSCs form bone

The rat femoral gap model was established and optimized by Stevenson, Einhorn and others [11, 33, 34]. This model is a critically-sized segmental defect that allows for the investigation of bone repair of cell-loaded implants in an orthotopic site using either immunocompromised or immunocompetent animals. In the first experiment, bone marrow from Fischer 344 rats was used to isolate and expand mesenchymal stem cells for syngeneic implantation [35]. At the end of the first passage, MSCs were subjected to an *in vitro* osteogenesis assay. Rat MSCs exposed to osteogenic supplements developed a cuboidal morphology and strongly expressed alkaline phosphatase by 21 days, and formed extensive mineralized bone nodules at the 28 day time point.

Porous HA/TCP (60% hydroxyapatite : 40% tricalcium phosphate) hollow cylinders were machined to fit into the rat femoral diaphyseal defect (4 mm outer diameter $\times$ 3 mm inner diameter $\times$ 8 mm length). Following sterilization and fibronectin coating, freshly trypsinized rat MSC suspensions (7.5×10^6 mL) were used to load the cylinders. Additional scaffolds were loaded with medium alone, with all implants incubated for 2 h at 37 °C prior to implantation. A third study group involved immersion of the scaffold in washed bone marrow, with each implant loaded with bone marrow equivalent to that found in an entire femur (approximately 50×10^6 cells). The final group investigated healing in the femoral gap in the absence of any implant material or cells. All implants were then placed in 8-mm defects created in the diaphysis of Fischer 344 rats using plate fixation.

Histological analysis of the explanted tissue was performed at 4 and 8 weeks post-implantation. At both time points, fibrous tissue was found in the empty defects; no bridging of the gap occurred. For cell-free HA/TCP implants, only fibrous tissue filled the pore space of the central region of the implant at both time points (Figs. 1(a) and (b)). Some bony integration with the host was present, and was estimated to be due to the limited extent of host cell migration into the implant. Similarly, small amounts of bone were present at 4 and 8 weeks in the marrow-loaded implants (Figs. 1(e) and (f)). Bone was limited to the pore spaces at the ends of the implants, adjacent to the host bone tissue.

MSC-loaded implants demonstrated a striking difference, with more than double the extent of bone formation present in the other study groups at both time points. At 8 weeks, virtually every pore within the implants contained newly formed bone (Fig. 1(d)). With extensive bone formation between the host bone and implant, there was complete bridging of the gap, including periosteal callus development. Furthermore, complete vascularization of the new tissue demonstrated the abundant neovascular-

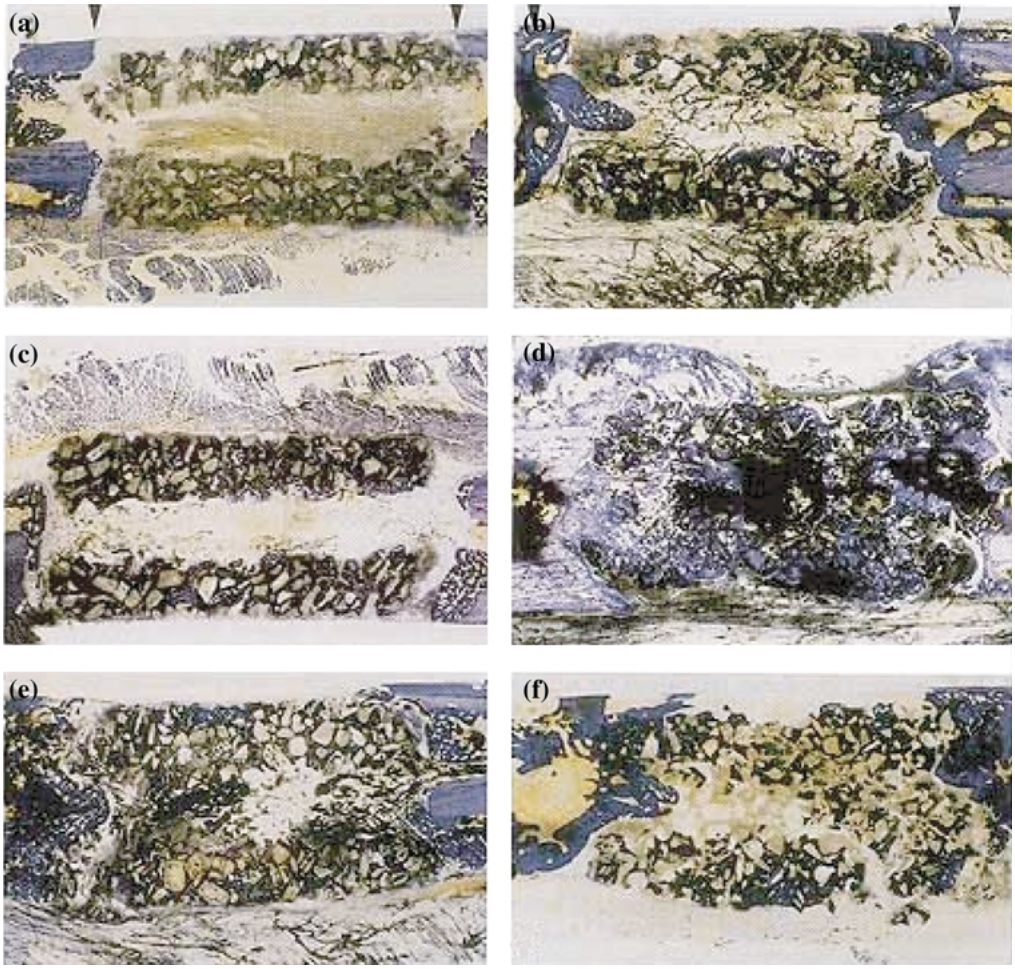

Figure 1 Histological micrographs of undecalcified longitudinal sections of rat segmental defects treated with (a,b) HA/TCP ceramic alone, (c,d) MSC-loaded HA/TCP, and (e,f) marrow-loaded HA/TCP at 4 and 8 weeks post-implantation, respectively (toluidine blue, 8 × magnification). Some animals received India ink injections to allow for visualization of the vascular tree, present here in (a) and (c) as black staining. Bone appears blue and ceramic appears black. Only implants containing MSCs effectively healed the defect, as noted by the extensive amount of bone present within the implant and at the interface of the host in (c) and (d) (published in Tissue Engineering [35]).

ization that paralleled bone regeneration. The percentage of bone fill in the pore space, as measured by histomorphometry, also confirmed that significantly more bone was present in the MSC-loaded implants than the marrow-loaded and cell-free implants for both time points ($p < 0.05$). MSC-loaded implants had $19.3 \pm 3.7\%$ and $43.3 \pm 7.7\%$ percent bone fill at 4 and 8 weeks, respectively. Marrow-loaded implants had $2.9 \pm 1.7\%$ and $17.2 \pm 6.0\%$ bone fill and cell-free implants had $2.3 \pm 1.5\%$ and $10.4 \pm 2.4\%$ bone fill at 4 and 8 weeks, respectively.

Confident that rat MSC-HA/TCP implants were effective in regenerating bone in this critically-sized model, subsequent studies were performed focusing on the use of human MSCs in an equivalent model [36]. Identical HA/TCP implants were loaded with human MSCs and medium alone and incubated for 2 h at 37 °C prior to implantation. To investigate human cells, Harlan Nude (Hsd:Rh-rnu) rats were subjected to the femoral gap described above. Implants were placed, with one limb receiving a MSC-loaded implant and the contralateral limb receiving a cell-free scafffold. Radiographic, histological, and mechanical analysis was used to evaluate the regenerative capacity of the human MSCs.

Osteogenesis was apparent at 4 weeks following implantation in the human MSC-loaded implants, but was absent in the cell-free implants. At 8 weeks, the MSC-loaded implants were well integrated with the host as evidenced in the radiodense bridging between the host and the MSC-implants. The bridging increased in radioopacity by 12 weeks and was concurrent with callus formation spanning the defect (Fig. 2). For cell-free implants, osteoconduction from the host led to reactive bone formation at the interface region only. Histological evaluation demonstrated significantly more bone fill in MSC-loaded implants compared to cell-free implants at both 8 and 12 weeks, as determined by paired *t*-tests for $p < 0.05$. At 8 weeks, the percentage of bone fill was 22.88 ± 4.25 and 12.95 ± 5.35 for the cell-loaded versus cell-free implants, respectively. At the 12 week time point, the cell loaded implant had nearly 50% (45.77 ± 14.56) of the pore space filled with newly formed bone versus $30.28 \pm 10.18\%$ percent for the cell-free implant. Most promising were results from mechanical testing where limbs treated with MSC-loaded implants had statistically greater strength and stiffness values as compared to limbs treated with the scaffold alone ($p < 0.05$). Strength values for MSC-loaded and cell-free implants measured at 12 weeks post-implantation were 159 ± 37 and 74 ± 63 N mm, respec-

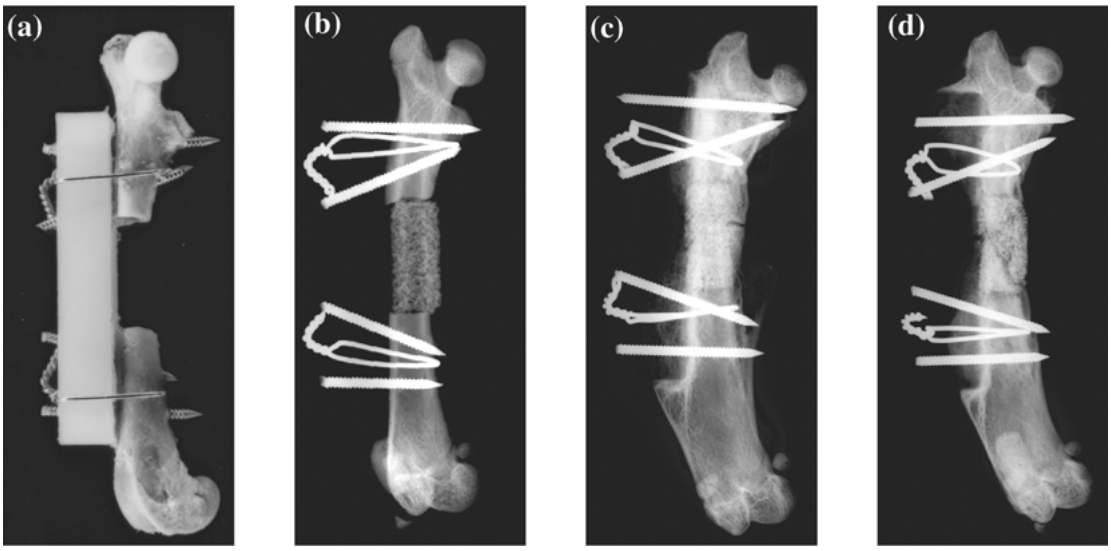

Figure 2 Radiographs of rat femoral defects (a) prior to implantation, (b) immediately post-implantation, (c) treated with HA/TCP loaded human MSCs at 12 weeks post-implantation and (d) treated with HA/TCP alone at 12 weeks post-implantation. For the limbs treated with MSCs, a large callus spanned the entire length of the defect on the medial aspect (opposite of the plate) of the limb, bony union occurred at both proximal and distal interfaces, and there was increased radioopacity evident in the implants, indicative of mineralized tissue. For cell-free HA/TCP implants, fracture lines occurred throughout the implant and implants appeared porous (published in Journal of Orthopaedic Research [36]).

tively. The corresponding stiffness values for the MSC-loaded and cell-free implants were 16.2 ± 4.0 versus 6.6 ± 4.2 N mm/deg, respectively.

The results from these two studies demonstrated complete bony bridging of critically-sized defects upon implantation of MSCs, either rat or human, using an HA/TCP scaffold. The aim of the subsequent study focused on a clinically relevant, large animal defect model, in addition to investigating the feasibility for production of an autologous MSC product.

Canine femoral gap

To develop a clinically applicable product, it was evident that shipment of bone marrow and isolation of mesenchymal stem cells at a separate facility may be necessary. To mimic this scenario, bone marrow samples were drawn from the iliac crest of large mongrel hounds at Tuft's University (Connecticut), and shipped to Osiris Therapeutics, Inc. in Baltimore, MD. MSCs were then isolated and expanded from each donor [37]. The osteogenic potential of each donor was verified through subcutaneous implantation of MSCs loaded onto HA/TCP.

The canine femoral gap defect was then used to demonstrate MSC-mediated bone formation in a large animal model. MSCs were loaded onto 60/40 HA/TCP porous scaffolds custom milled into hollow cylinders to closely approximate the defect dimensions. The implants were then shipped to the surgical facility for implantation. A 21-mm osteoperiosteal defect was created unilaterally in the mongrel hounds. Implants were implanted in an autologous manner, with cell-free HA/TCP implants and autograft bone segments serving as controls. Additional animals were subjected to the surgical procedure and the defects remained empty throughout the experimental period.

Implants were investigated radiographically throughout the in-life period, with histological analysis performed at sacrifice. Empty defects showed a small amount of reactive bone formation at the periphery of the defect, but lacked bridging at all time points. Upon sacrifice at 16 weeks, the empty defects were filled with loose connective tissue, confirming the defect as critically-sized. Cell-free HA/TCP implants remained in the defect site, though many of the implants had fractured due to the transfer of load through the defect site. Callus was absent at all time points. Histological analysis of the cell-free implants showed reactive bone formation at the defect edges, but the center of the implants remained free of bone throughout the experiment. Defects filled with autologous bone demonstrated bridging of the space as early as 8 weeks, and corticalization at 16 weeks. Histological appearance of the autograft was reminiscent of remodeling bone in either development or fracture healing. The MSC-loaded HA/TCP implants were similarly encased in callus by 8 weeks post-implantation. The callus, characteristic of typical fracture repair, remodeled and the implant resembled cortical bone at 16 weeks (Fig. 3). All pore spaces demonstrated bone formation, completely bridging the defect with full integration of the implant with the host at each periphery. Histomorphometric analysis showed significantly more percent bone in MSC-loaded implants (39.9 ± 6.1) than in cell-free implants (24 ± 15.5), for $p < 0.05$.

Thus, this study confirmed the feasibility of bone marrow harvesting, MSC isolation and bone formation for autologous MSC implantation. Limitations of the HA/TCP scaffold however were (1) the lack of remodeling/resorption of the ceramic, which in turn limited the rate of bony integration, (2) its brittle mechanical properties. For this reason, experiments were designed to investigate fully resorbable scaffolds. One approach to enhance HA/TCP resorption is by varying the ratio of HA to TCP in the scaffold material.

Ceramic evaluation

The rate of degradation or resorption of HA/TCP ceramics *in vivo* can be accelerated by increasing the

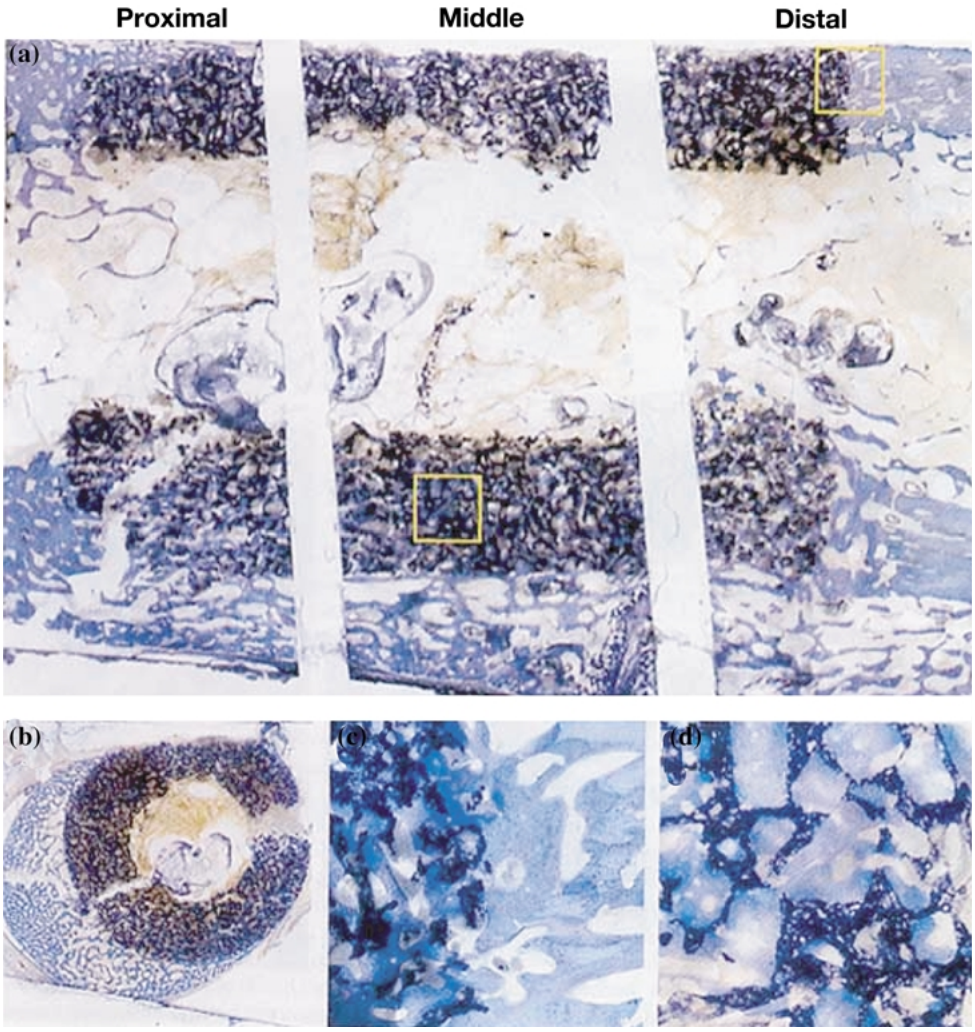

Figure 3 Histological micrographs of an undecalcified section of a segmental defect in the canine treated with HA/TCP loaded with autologous canine MSCs at 16 weeks post-implantation (toluidine blue stain). Bone appears blue and ceramic appears black (a) Longitudinal section showing the proximal host bone-implant interface, middle, and distal aspect of the defect along with host cortices (7 × magnification). The implantation of autologous MSCs led to the development of a large callus around the implant and bone formation throughout the porous space of the implant. (b) Cross-section that was obtained between the proximal host bone-implant interface and the middle portion of the implant (3 × magnification). The areas within the boxes in the distal and middle sections are shown at higher magnification (35 ×) in (c) and (d), respectively. (published in Journal of Bone and Joint Surgery [37]).

amount of the more soluble phase, TCP [38]. In order to design a scaffold that supports bone formation while gradually becoming replaced by bone, an optimum balance between the more stable phase (HA) and the more soluble phase (TCP) must be achieved. The goal of this study was to determine the optimal HA/TCP ratio seeded with MSCs that promoted rapid and uniform bone formation *in vivo*. To this end, human MSCs were evaluated on various HA/TCP compositions in an ectopic model in immunocompromised mice [39].

Six calcium phosphate ceramic compositions were examined: 100% Hydroxyapatite (100 HA), 100% β-tricalcium phosphate (100 TCP) and four formulations of HA/TCP (76/24, 63/37, 56/44 and 20/80, ratio of wt %HA/wt %TCP, Biomatlante, France). All compositions were manufactured with a porosity of 60–70% and a pore size range of 300–600 μm. Ceramics were milled into cubes having the dimensions of 3 mm × 3 mm × 3 mm, washed and sterilized by depyrogenation prior to cell seeding. Bone marrow was collected from two donors and human MSCs were isolated, culture expanded and cryopreserved as previously described. Thawed cells were then loaded onto scaffolds at 5×10^6 cells/mL using a vacuum technique. MSC-loaded implants and cell-free implants were implanted subcutaneously in the back of SCID mice. Implants were harvested at 6 and 12 weeks and processed for routine decalcified histology.

More bone formed within the pores of MSC-loaded 20/80 HA/TCP than all other implants at 6 weeks. By 12 weeks, MSC-loaded 56/44 and 20/80 HA/TCP demonstrated the greatest amount of bone and were equivalent to each other. The least amount of bone formed within the pores of 100 TCP and 100 HA throughout the study. These results demonstrated the potential of using faster resorbing ceramics, 56/44 and 20/80 HA/TCP, in combination with MSCs for bone regeneration. Future studies will test these results in more clinically relevant models.

Allogeneic MSCs for bone repair

For clinical application, the utility of a tissue engineering product will ultimately depend upon expedient delivery and cost-effectiveness. In an autologous setting, bone marrow would be harvested from the patient, MSCs

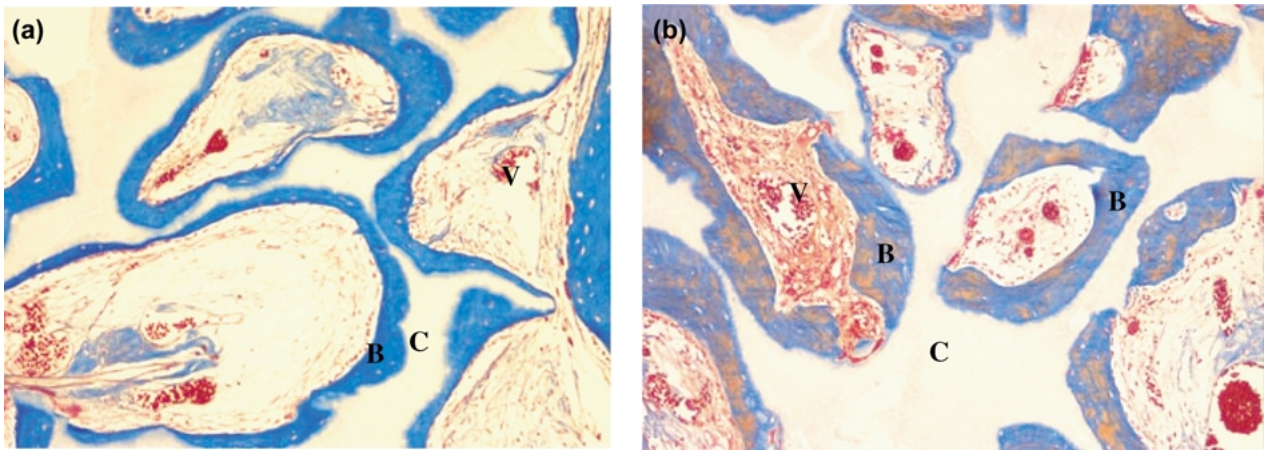

Figure 4 Histological micrographs of decalcified, paraffin embedded sections of implants in the mandibular defect model at 9 weeks post-implantation (200 × magnification, modified analine blue stain). For both the (a) autologous and (b) allogeneic groups, bone (B), which appears blue and red, lined the porous space of HA/TCP ceramic (C), which appears grayish-white. Blood vessels (V) were clearly distinguishable and there was a lack of inflammatory cell infiltrate for both groups.

expanded in culture and then administered back to the patient. Culture preparation per patient upon request increases production time and costs and in turn, cost to the patient. In addition, a patient has to wait weeks for MSC expansion prior to treatment. An attractive alternative is an allogeneic approach. MSCs are obtained from a donor, expanded and cryopreserved until use. Frozen cells are then thawed and seeded onto scaffolds for implantation, providing an ''off-the-shelf'' product to the patient. Since the donor and recipient could be completely unrelated/mismatched, the issue of immune reactivity or possible rejection arises. Previous analysis by flow cytometry has demonstrated that MSCs do not express MHC Class II molecules or the costimulatory molecules (B7, CD40) required to fully activate T cells responsible for transplant rejection [40, 41]. Furthermore, T cells are not activated when they are cultured with allogeneic MSCs, even when the MSCs have been induced to differentiate into osteoblasts (unpublished data). When these same T cells are cultured with irradiated peripheral blood cells from the MSC donor, a vigorous response was elicited. Interestingly, when MSCs are added to a vigorous mixed lymphocyte culture, they suppress it [40, 41]. The combination of a cell phenotype showing low immunogenicity coupled with a suppressive activity allow the MSCs to avoid rejection upon allogeneic implantation. The aim of our current studies is to demonstrate that allogeneic MSCs do not provoke an adverse immune response and can enhance bone repair.

Constructs containing allogeneic MSCs on HA/TCP ceramic were investigated in the augmentation and repair of alveolar bone in a canine model. Allogenecity or the extent of mismatch between donor and recipient dogs was determined by three techniques: pedigree, mixed lymphocyte reaction (MLR) assay, and dog leukocyte antigen (DLA) typing. Under general anesthesia, the second, third and fourth premolar teeth were extracted bilaterally by bisection and elevation from adult beagle dogs. Seven weeks following extractions, a midcrestal incision was made and full thickness mucoperiosteal flaps were elevated from the first premolar to the first molar teeth. Saddle defects (6.5 mm deep × 20 mm long) were created bilaterally in the mandible of each dog. Porous 60/40 HA/TCP implants, 6 mm width × 6 mm length × 20 mm height, with a 3 mm diameter longitudinal central canal, were loaded with autologous MSCs, allogeneic MSCs, or loaded with cell-free medium and placed into the defects. All implants were secured with wire and covered with a PTFE membrane to exclude periosteal contribution to repair. At 4 and 9 weeks post-implantation, the tissue response in the implants was examined histologically. The humoral allo-antibody response to implanted MSC-loaded implants was evaluated by flow cytometric analysis, similar to methods used to evaluate human panel reactive antibody (PRA) levels [42] at 4 and 9 weeks post-implantation.

At the 4 week time point, for all groups, the presence of granulation tissue and vasculature, which is typically associated with the early stages of bone repair, was detected in the porous space of the implants. There was no evidence of a lymphocytic infiltrate in any group at this time point. By 8 weeks, bone was present throughout the porous spaces of the ceramics for both autologous and allogeneic MSC groups (Fig. 4). At 9 weeks, the cell-free implants consisted mostly of fibrous tissue. No adverse cellular immune response was detected histologically for any group including the allogeneic MSC group. In addition, antibodies to donor allo antigens were not detected in the host serum at 4 and 9 weeks post-implantation. Both autologous and allogeneic cells were fluorescently labeled prior to implantation and were detected within the bone and lining tissue at 9 weeks post-implantation (Fig. 5). This model was a first study to examine the allogeneic approach to MSC induced bone repair and demonstrated allogeneic MSCs did not provoke an adverse immune response and maintained the capacity to promote bone repair.

Future directions

Mesenchymal stem cell-based bone regeneration has been demonstrated in various animal models. Use of this therapy in the clinic has begun in a Phase I clinical trial applying autologous MSCs to a 60/40 HA/TCP scaffold

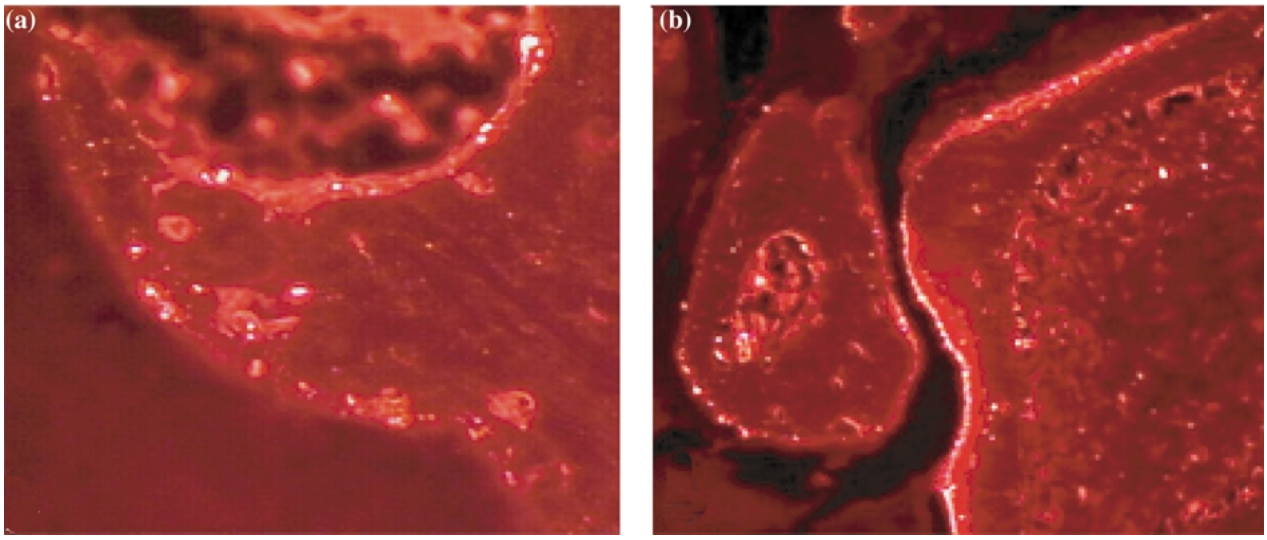

Figure 5 Histological micrographs of fluorescently labeled (a) autologous and (b) allogeneic cells at 9 weeks post-implantation in the canine mandibular defect model (200 × magnification). Di-I labeled cells appear bright white against the light red new matrix or dark red mineralized bone tissue. Labeled cells were detected embedded in newly forming matrix as well as the lining the surface of the bone tissue.

for dental applications. Additional preclinical studies to evaluate the safety and efficacy of allogeneic MSC-based bone formation are being conducted. In addition, scaffold materials have been varied beyond those described here to explore their utility in cell-based engineering of bone.

Acknowledgments

The authors thank Jerry Skwarek for his histological expertise and Heather Spencer, Randell Young, and Jim Cole for their contributions in animal handling and surgical procedures. Lastly, the authors thank Mohammad ElKalay for his assistance in completing the early experiments described. This work was partially sponsored through generous grants from National Institutes of Health and the National Institutes of Standards and Technology.

References

1. M. F. PITTENGER, A. M. MACKAY, S. C. BECK, R. K. JAISWAL, R. DOUGLAS, J. MOSCA, M. A. MOORMAN, D. W. SIMONETTI, S. CRAIG and D. R. MARSHAK, *Science* **284** (1999) 143.
2. A. I. CAPLAN, D. J. FINK, T. GOTO, A. E. LINTON, R. G. YOUNG, S. WAKITANI, V. GOLDBERG and S. E. HAYNESWORTH, in ''The Anterior Cruciate Ligament: Current and Future Concepts'' (Raven Press, New York, 1993) p. 405.
3. N. JAISWAL, S. E. HAYNESWORTH, A. I. CAPLAN and S. P. BRUDER, *J. Cell. Biochem.* **64** (1997) 295.
4. A. FRIEDENSTEIN, R. CHAILAKHYAN and U. V. GERASIMOV, *Cell Tissue Kinet.* **20** (1987) 263.
5. D. P. LENNON, S. E. HAYNESWORTH, S. P. BRUDER, N. JAISWAL and A. I. CAPLAN, *In Vitro Cell. Dev. Biol. Animal* **32** (1996) 602.
6. J. N. BERESFORD, *Clin. Orthop.* **240** (1989) 270.
7. S. HAYNESWORTH, M. BABER and A. CAPLAN, *J. Cell. Physiol.* **138** (1992) 8.
8. S. KADIYALA, R. G. YOUNG, M. A. THIEDE and S. P. BRUDER, *Cell Transplan.* **6** (1997) 125.
9. M. J. YASZEMSKI, R. G. PAYNE, W. C. HAYES, R. LANGER and A. G. MIKOS, *Biomaterials* **17** (1996) 175.
10. A. GAZDAG, J. LANE, D. GLASER and R. FORSTER, *J. Am. Acad. Orthop. Surg.* **3** (1995) 1.
11. X. LI, S. STEVENSON, L. KLEIN, D. DAVY, J. SHAFFER and V. GOLDBERG, *Acta Anat. Basel* **140** (1991) 236.
12. D. EHRLER and A. VACCARO, *Clin. Orthop.* **371** (2000) 38.
13. W. HEAD, T. MALININ, T. MALLORY and R. EMERSON, *Orthop. Clin. North Am.* **29** (1998) 307.
14. A. AHO, T. EKFORS, P. DEAN, H. ARO, A. AHONEN and V. NIKKANEN, *Clin. Orthop.* **307** (1994) 200.
15. D. GARBUZ, B. MASRI and A. CZITROM, *Orthop. Clin. North Am.* **29** (1998) 199.
16. L. L. HENCH, *J. Am. Ceram. Soc.* **74** (1991) 1487.
17. E. C. SHORS, *Orthop. Clin. North Am.* **30** (1999) 599.
18. R. Z. LEGEROS, *Adv. Dental Res.* **2** (1988) 164.
19. P. PATKA, G. DEN OTTER, K. DE GROOT and A. DRIESSEN, *Neth. J. Surg.* **37** (1985) 38.
20. G. DACULSI, N. PASSUTI, S. MARTIN, C. DEUDON, R. Z. LEGEROS and S. RAHER, *J. Biomed. Mater. Res.* **24** (1990) 379.
21. M. MARCACCI, E. KON, S. ZAFFAGNINI, R. GIARDINO, M. ROCCA, A. CORSI, A. BENVENUTI, P. BIANCO, R. QUARTO, I. MARTIN, A. MURAGLIA and R. CANCEDDA, *Calcif. Tissue. Int.* **64** (1999) 83.
22. K. JOHNSON, K. FRIERSON, T. KELLER, C. COOK, R. SCHEINBERG, J. ZERWEKH, L. MEYERS and M. SCIADINI, *J. Orthop. Res.* **14** (1996) 351.
23. C. FRIEDMAN, P. COSTANTINO, C. SYNDERMAN, L. CHOW and S. TAKAGI, *Arch. Facial Plast. Surg.* **2** (2000) 124.
24. O. GAUTHIER, J. M. BOULER, E. AGUADO, P. PILET and G. DACULSI, *Biometerials* **19** (1998) 133.
25. E. J. G. SCHEPERS and P. DUCHEYNE, *J. Oral Rehab.* **24** (1997) 171.
26. Y. MATSUSUE, T. KOTAKE, Y. NAKAGAWA and T. NAKAMURA, *Arthroscopy* **17** (2001) 653.
27. D. BUSER, B. HOFFMANN, J. BERNARD, A. LUSSI, D. METTLER and R. SCHENK, *Clin. Oral. Implants Res.* **9** (1998) 137.
28. K. HAMSON, J. TOTH, J. STIEHL and K. LYNCH, *Calcif. Tissue Int.* **57** (1995) 64.
29. H. OHGUSHI, Y. DOHI, T. YOSHIKAWA, S. TAMAI, S. TABATA, K. OKUNAGA and T. SHIBUYA, *J. Biomed. Mater. Res.* **32** (1996) 341.
30. J. TOQUET, R. ROHANIZADEH, J. GUICHEUX, S. COUILLAUD, N. PASSUTI, G. DACULSI and D. HEYMANN, *ibid.* **44** (1999) 98.
31. T. LIVINGSTON, P. DUCHEYNE and J. GARINO, *ibid.* (2002) in press.
32. S. HAYNESWORTH, J. GOSHIMA, V. GOLDBERG and A. CAPLAN, *Bone* **13** (1992) 81.
33. T. A. EINHORN, J. M. LANE, A. H. BURSTEIN, C. R. KOPMAN and V. J. VIGORITA, *J. Bone Joint Surg. Am.* **66-A** (1984) 274.
34. M. NOTTEBAERT, J. M. LANE, A. JUHN, A. BURNSTEIN, R.

SCHNEIDER, C. KLEIN, R. S. SINN, C. DOWLING, C. CORNELL and M. CATSIMPOOLAS, *J. Orthop. Res.* **7** (1989) 157.
35. S. KADIYALA, N. JAISWAL and S. P. BRUDER, *Tiss. Eng.* **3** (1997) 173.
36. S. P. BRUDER, A. A. KURTH, M. SHEA, W. C. HAYES, N. JAISWAL and S. KADIYALA, *J. Orthop. Res.* **16** (1998) 155.
37. S. P. BRUDER, K. H. KRAUS, V. M. GOLDBERG and S. KADIYALA, *J. Bone. Joint Surg.* **80-A** (1998) 985.
38. G. DACULSI, *Biomaterials* **19** (1998) 1473.
39. T. L. LIVINGSTON, G. DALCUSI, M. ELKALAY and S. KADIYALA, *Am. Soc. Artificial Internal Organs J.* **46** (2000) 238.
40. K. MCINTOSH and A. BARTHOLOMEW, *Graft* **3** (2000) 324.
41. S. DEVINE, S. PETER, B. J. MARTIN, F. BARRY and K. MCINTOSH, *Cancer J.* **7** (2001) S76.
42. W. E. BRAUN, *Am. J. Med. Sci.* **313** (1997) 279.

Received 31 July
and accepted 31 October 2002